





Benchmarking of Heuristic Algorithms for Energy Router-Based Packetized Energy Management in Smart Homes

Hafiz Majid Hussain , Ashfaq Ahmad , *Member, IEEE*, Arun Narayanan , *Member, IEEE*, Pedro H. J. Nardelli , and Yongheng Yang , *Senior Member, IEEE*

Abstract—This article presents an ER-based PEM strategy for PV integrated smart homes to jointly optimize their load scheduling delays, energy transactions cost, and battery degradation cost. The proposed approach incorporates a MA case, where, the ER acts as a main selecting agent realized by all other system elements. This leads to a combinatorial optimization problem, which can be effectively solved by heuristic optimization methods (HOMs), namely, genetic algorithm (GA), binary particle swarm optimization (BPSO), differential evolution (DE) algorithm, and harmony search algorithm (HSA). Specifically, we investigate the impact of the hyperparameters of the HOMs on the designed ER-based PEM system. Simulations are carried out for multiple smart homes under varying weather conditions to evaluate the effectiveness of HOMs in terms of selected performance metrics. Results show that the ER-based PEM reduces the average aggregated system cost, ensures economic benefits by selling surplus energy, while meeting customers energy packet demand, satisfying their quality-of-service, and operational constraints.

Index Terms—Energy Internet (EI), energy router (ER), heuristic algorithms, packetized energy management systems (PEMs).

NOMENCLATURE

Abbreviations

DMS	Demand-side management.
EI	Energy Internet.
ER	Energy router.
PV	Photovoltaic.
EMS	Energy management system.

Manuscript received 4 March 2022; revised 27 June 2022 and 31 August 2022; accepted 8 September 2022. This work was supported in part by the Academy of Finland via FIREMAN consortium 326270 as part of CHIST-ERA under Grant CHIST-ERA-17-BDSI-003, in part by EnergyNet Fellowship321265/328869/352654, and X-SDEN under Project 349965, and in part by Baltic-Nordic Energy Research programme via Next-uGrid under Project 117766. (*Corresponding author: Hafiz Majid Hussain.*)

Hafiz Majid Hussain, Arun Narayanan, and Pedro H. J. Nardelli are with the Department of Electrical Engineering, Lappeenranta University of Technology, 53850 Lappeenranta, Finland (e-mail: majid.hussain@lut.fi; arun.narayanan@lut.fi; Pedro.Nardelli@lut.fi).

Ashfaq Ahmad is with the Department of Electrical and Computer Engineering, Air University, Islamabad 44000, Pakistan (e-mail: ashfaqahmad@ieec.org).

Yongheng Yang is with the College of Electrical Engineering, Zhejiang University, Zhejiang 310027, China (e-mail: yang_yh@zju.edu.cn).

Digital Object Identifier 10.1109/JSYST.2022.3208414

MAs	Multiagents.
PEM	Packetized energy management system.
P-ESP	Packetized energy service provider.
PEC	Packetized energy cost.
PLC	Power line communication.
RRs	Renewable resources.
QoS	Quality-of-service.
SDN	Software-defined network.

Indices and Superscripts

t	Time step.
max	Maximum.
min	Minimum.
—	Average.
'	Derivative.
i	Superscript for load from 1 to N .
j	Superscript for smart home from 1 to M .
t	Superscript for time period from 1 to T_0 .
r	Subscript for particle in the swarm.

Main Symbols

C_{bt}	Crossover operator.
M_{bt}	Mutation operator.
$d_t^{j,i}$	Delay experienced by a load i in a smart home j at time t .
$E_{t,pv}^j$	Harvested amount of PV energy by a smart home j at t .
$E_t^{j,s}$	Battery state of energy of a smart home j at t .
$P_t^{j,i}$	Energy packets demand by a smart home j at t .
$P_{T_0}^{M,N}$	Total energy packets demanded by M smart homes of N loads over T_0 .
E_t^g	Energy packets supplied by utility grid.
$H_t^{j,buy}$	Energy packets procured by a smart home j from E_t^g .
$H_t^{j,sell}$	The E packets sold by a smart home j to E_t^g .
$R_t^{DS,j}$	Demand-and-supply ratio at time t .
J_t^{buy}	$P_t^{j,i}$ procured by P-ESP from E_t^g at t .
J_t^{sell}	$P_t^{j,i}$ sold by P-ESP to utility grid at t .
$K_d \left(\bar{d}_{T_0}^{M,N} \right)$	Cost function based on average delay experienced by M smart homes M of N loads over T_0 .
$K_t^{j,buy}$	Cost of $P_t^{j,i}$ buying by j from utility grid at t .

$K_t^{j,buy}$	Cost of $P_t^{j,i}$ selling by j from utility grid at t .
$\overline{K}_{T_0}^{M,tx}$	Average cost associated with the transactions of energy packets for M smart homes over T_0 .
$\overline{K}_{T_0}^{M,s}$	Average cost associated with charging and discharging activities for M smart homes over T_0 .
$x_t^{j,i}$	Time slots available for scheduling of $P_t^{j,i}$.
$P_{t,min}^{j,i}$	Lower bound of the $P_t^{j,i}$.
$P_{t,max}^{j,i}$	Upper bound of the $P_t^{j,i}$.
B_{max}	Upper bound of J_t^{buy} .
$E_t^{j,s}$	Amount of energy charged in a storage system of a smart home at t .
k_t^j	Amount of energy discharged from storage system of a smart home at t .
$E_{t,max}^{j,s}$	Per slot upper bound on amount of energy charged in storage system by a smart home at t .
k_{max}^j	Per slot upper bound on amount of energy discharged in a smart home at t .
$E_{min}^{j,s}$	Per slot minimum required $E_t^{j,s}$ for a storage system.
$E_{t,pv}^j$	Amount of energy harvested from PV by a smart home.
$c_t^{j,(+)}$	Admission cost for the charging event of a storage system in a smart home at t .
$c_t^{j,(-)}$	Admission cost for the discharging event of a storage system in a smart home at t .
$E_{t,pv}^{j,c}$	Consumed portion of PV energy stored by j at t .
$E_{t,pv}^{j,r}$	Residual portion of PV energy by smart home in the battery at t .
$E_{T_0,pv}^M$	Amount of energy produced by PV panel for all smart homes M over T_0 .
S_{max}	Upper bound on the total amount of energy stored in a battery.

I. INTRODUCTION

OVER the past few decades, electric power system has been influenced greatly by the integration of large-scale RRs. The RRs (represented by solar panels and wind turbines) have become inevitable for alleviating energy prices and mitigating environmental concerns [1], [2]. Yet, energy generation from RRs is intermittent making them less reliable for a stable operation of the power system [3]. Recently, EI has been widely investigated to combat the intermittency in renewable generation through Internet-oriented technologies, such as ERs, plug and play services, and PEM [4], [5], [6].

In the EI paradigm, ER is an integral part, analogous to a router in an Internet network [7]. ER provides real-time communication among users and the utility grid and performs management of RRs, flexible and nonflexible household loads, rooftop PV panels, and storage system often classified as *agents* [8]. Thus, ER is regarded as an essential element that interfaces multiple agents (MAs) and enables energy resource allocation in smart homes exploiting demand-side management (DSM) [9], [10].

PEM as a part of the DSM can be utilized to meet energy packet demand of smart home customers by scheduling flexible energy packets while ensuring their QoS constraints [11]. In PEM, energy is delivered to the customer loads in the form of energy packets that represent fixed power consumed by the load during a predefined time interval, e.g., 1 kW in an hour [12]. In this sense, this article focuses on the ER-based PEM (ER-PEM) framework for smart homes and provides resource allocation of MAs operating at various times instants. In addition, ER-PEM enables cost-effective solutions for smart users considering QoS, energy transactions between ER and utility grid, PV energy, and storage system.

However, a limited amount of work has been done in the above context and most of the literature has either focused on communication and control aspects [5], [6], [7], [9], [13] or on energy management aspects of ER [11], [12], [14], [15], [16], [17], [18], [19], [20], [21], [22], [23]. For instance, authors in [5] and [6], described the role of the ER in EI networks, investigated design challenges in terms of communication typologies, governance models, and security concerns. Gao et al. [7] studied an ER-based system to investigate the communication and reliability of multiple ERs and energy trading for green cities in EI. Guo et al. in [9] proposed secure energy routing protocols for the optimal energy dispatch between energy hubs (EH) considering power transmission constraints in the EI. Tu et al. [13] proposed a modular-based ER strategy for connecting dc micro grid clusters with ac grids. The other references investigated the operation of ER based on the management aspects [11], [12], [14], [15], [16], [17], [18], [19], [20], [21], [22], [23], for example, authors in [11] and [12] evaluated the QoS metric for load allocation problem using PEM system. Li et al. [14] proposed an optimization-based strategy for the integrated energy system to minimize the cost of the EH using ER applications. In [15], the authors examined optimization problems for home energy management systems (HEMS) in the context of the EH, while the authors in [16] and [17] formulated an energy management solution for operational costs and CO₂ minimization considering contingency constraints in microgrids. Ahmad and Khan [18] solved the joint optimization problem through Lyapunov optimization considering renewable sources, loads, and energy procurement prices, whereas Carli et al. in [19] proposed scheduling algorithms for solving an online optimization problem in microgrids and daily cost minimization through the DSM was achieved. Demand response (DR) methods were proposed in [20] and [21] to control the peak to average ratio (PAR) and to reduce systems costs, while the authors in [22] and [23] investigated HEMS with DSM to reduce energy costs and peak power consumption, considering user's requirements over a finite time horizon.

It is suggested from the above literature review that most of the previous works have investigated energy management solutions e.g., [16], [17], [18], [19], [20], [21], [22], [23] or the control and routing aspects of the ER [7], [9], [15] without considering distinctive and key aspects of EI, such as ER, MAs, and PEM. Although authors in [11] and [12] have studied PEM-based solutions, however, their system model has not provided

TABLE I
COMPARISON OF THE STATE-OF-THE-ART WORKS WITH OUR DESIGNED SYSTEM MODEL

S.Nr	Ref.(s)	Method (s)	Energy premises	PEM System	Use of RRs	Contribution(s)
1	[7]	Hierarchical optimization strategy	Smart energy community	NO	YES	To minimize daily operational cost of EH considering the energy transaction of EHs in EI.
2	[9]	Markov decision process	Smart energy community	NO	NO	To control and verify the energy transmission and management of ER-based system.
3	[11]	Rule based optimization	Smart homes	YES	NO	To reduce peak shaving.
4	[12]	Controlled Markov chain	Smart home	YES	YES	To obtain QoS for managing RRs via PEM.
5	[15]	Probabilistic optimization approach	Smart home	NO	YES	To minimize the energy cost of the customer.
6	[16]	MINLP	Microgrid	NO	YES	To achieve the optimal day-ahead scheduling of energy resources.
7	[17]	Lightning search optimization algorithm	Microgrid	NO	YES	To minimize the aggregated operational cost of the system.
8	[18]	Lyapunov optimization technique	Smart building	NO	YES	To minimize the aggregated average operation cost of the system.
9	[19]	Model Predictive Control	Smart building	NO	YES	To minimize the daily cost of the energy from the main grid.
10	[20], [23]	Heuristic optimization algorithms	Smart home	NO	YES	To minimize the cost of the smart home and reduce PAR.
11	[21]	Artificial immune algorithm	Smart energy community	NO	YES	To maximize the net profit by decreasing the operating cost of the system.
12	[22]	Natural aggregation optimization algorithm	Smart energy community	NO	YES	To minimize one day cost of the smart home and reduce PAR.
14	<i>Our work</i>	Heuristic optimization algorithms	Smart energy community	YES	YES	To minimize aggregated average cost of system based on (a) energy packet transactions cost (b) load scheduling delays cost (c) battery degradation cost.

Research limitations in [7], [9], [11], [12], [15]–[23]: (i) The ER-PEM system including; the key attributes of EI such as ER, MAs, and PEM has seldom been explored in previous works [7], [9], [11], [12], [15]–[23]. (ii) Most of the studies have investigated the minimization of the system cost based on the various methods, however, their design system lack adequate analysis either on PEM system [15]–[23] or energy packets attributes e.g., arrival time, unit demand, scheduling start time, departure time, and allowable service delay [7], [9], [11], [12]. (iii) In addition, none of the previous works has provided comparative analysis of heuristic algorithms in the context of ER-based PEM system.

Research contributions: (i) This work presented a comprehensive ER-PEM system for multiple smart homes and their associated characteristics including energy packet attributes, delay constraints, PV energy generation, battery storage system, and energy packets transactions. (ii) ER-based PEM system solved the joint optimization problem of minimizing average aggregated system costs based on, energy packet transactions cost, load scheduling delays cost, and battery degradation cost (iii) The designed ER-PEM system also evaluated the comparative performance of heuristic algorithms and the impact of their hyperparameters on energy packet transactions and their associated service delays.

adequate analysis of design aspects of energy packets, for instance, arrival time, unit energy packet demand, scheduling start time, departure time, and allowable service delay. In contrast, the designed ER-PEM system is a unique architecture and incorporated distinctive design aspects of EI and ER-PEM system. Moreover, the designed ER-PEM system not only accomplished the objectives (i.e., to minimize average aggregated system costs based on, energy packet transactions cost, load scheduling delays cost, and battery degradation cost) but also carried a comparative analysis of the heuristic optimization methods (HOMs) in terms of different sets of hyperparameters and different seasons. Table I briefly summarizes the models in the previous work and also compares the previous models with the designed ER-PEM system in this article.

In the above context, we present an ER-PEM system for multiple smart homes to achieve optimal energy plans in terms of management of MAs based on heuristic optimization methods. Specifically, we account for key attributes of the smart homes, i.e., energy packet scheduling and pricing parameters, and constraints of roof-top panels and energy storage system in the context of ER-PEM system. The goal of ER-PEM is to minimize an average aggregated system cost by solving a joint optimization problem of load scheduling and storage management. The minimization of an average aggregated system cost is subject to constraints of energy demand,

scheduling delay parameters, storage system management and energy procurement parameters. To this joint optimization problem, we employ HOMs: genetic algorithm (GA), binary particle swarm optimization (BPSO), differential evolution (DE), and harmony search algorithm (HSA). Finally, we present simulation results and analyze the relative performance of HOMs and the impact of their hyperparameters on the designed ER-PEM system.

The major contributions of this work are summarized below.

- 1) A comprehensive system model is presented for smart homes based on an ER-PEM system. The model consists of multiple smart homes and their associated characteristics including energy packet attributes and delay constraints, PV energy generation, battery storage system, and energy packets' transactions.
- 2) An energy pricing model ([24], [25]) is tailored for energy packet exchange (buy and sell) between smart homes and packetized energy service provider (P-ESP). The model provides flexibility for economic energy transactions while conserving the demand–supply ratio.
- 3) The joint optimization problem is solved by implementing four well-known HOMs—GA, BPSO, DE, and HSA—and their performance and suitability for the designed system model are benchmarked.

- 4) A comprehensive case study is conducted to evaluate HOMs and their associated hyperparameters in terms average aggregated system cost parameters.

Note that this work is an extension of [26] and it contributes in the following ways.

- 1) Literature review is extensively updated with state-of-the-art research methods in terms of their contributions and potential research gaps.
- 2) Unlike a single smart home in [26], the ER- PEM model in this article is upgraded with a systematic integration of multiple smart homes, their respective attributes and constraints considering an extended set of HOMs and varying weather conditions.
- 3) The relative performance analysis of HOMs is carried out based on the joint optimization problem of load scheduling and storage management in the ER-PEM system.

In addition, simulation scenarios are extended to investigate the impact of the HOMs' hyperparameters on energy packet transactions and their associated service delays.

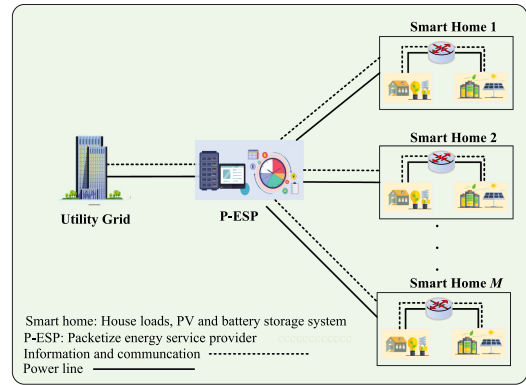
The rest of this article is organized as follows. Section II formulates the problem and provides the system model. A brief overview of heuristic optimization is given in Section IV. Simulation results are presented in Section V. Finally, Section VI concludes this article.

II. SYSTEM MODEL

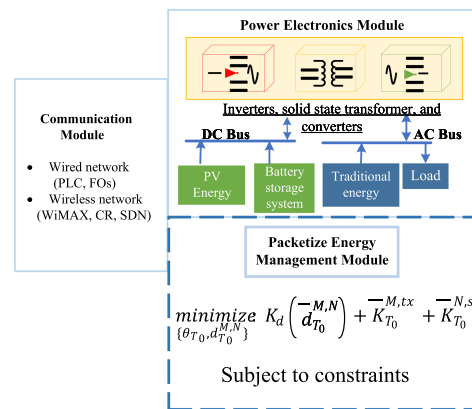
Fig. 1 depicts conceptual overview of ER-PEM system. Where Fig. 1(a) shows the interaction of ER with MAs, utility grid, and P-ESP, and Fig. 1(b) represents three main building blocks of the ER: a power electronics module, a communication module, and a management-and-control module [7]. The power electronics module can be a solid-state transformer, inverters, and converters to provide circuitry-based active control of energy flows. The management module is responsible for allocating energy resources and providing optimal energy usage plans to satisfy users' demand and cost requirements. The power electronics and management modules are connected through a communication module that may consist of a wired network, e.g., PLC and fiber optics (FOs), a wireless network, e.g., WiMAX, cognitive radio (CR), and a SDN, or a combination of both [5]. Potentially, the ER can act like a plug-and-play interface for smart homes to connect to or disconnect from traditional energy sources, PV sources, battery storage systems, and electrical loads. In this work, we mainly focus on packetized energy optimization via an energy management module carrying the following tasks: 1) devise and manage schedules for energy packets transactions considering all connected sources, storage, and loads; and 2) coordinate with the P-ESP for economic energy transactions.

A. Load Model

A set of smart homes $j \in \{1, 2, \dots, M\}$ accommodate loads $i \in \{1, 2, \dots, N\}$ that operate at discrete time slots $t \in \{0, 1, 2, \dots, T_0 - 1\}$ in a local energy community. The loads



(a)



(b)

Fig. 1. (a) Illustration of the ER-PEM system. (b) Main modules of an ER.

are energy consumption elements in each smart home, and they are characterized by different attributes as follows.

- 1) Load arrival time ($q_t^{j,i}$): The time slot at which a request for a given load arrives in a smart home j .
- 2) Unit energy packets demand ($P_t^{j,i}$): In a smart home, we consider the energy is consumed in the form of discrete value packets by load i and each energy packet is represented by $P_t^{j,i}$. Here, $P_t^{j,i} = \frac{P_e - P_{e-1}}{t_k - t_{k-1}}, \forall e \in \{1, 2, \dots, E\}$ and $\forall k \in \{1, 2, \dots, K\}$, as shown in Fig. 2.
- 3) Scheduling start time ($\zeta_t^{j,i}$): Time slot at which the load is actually scheduled.
- 4) Length of operation time ($\varsigma_t^{j,i}$): The number of time slots during which the load completes its operations.
- 5) Maximum allowable delay ($d_{t,\max}^{j,i}$): The maximum amount of delay (i.e., the number of time slots) that can be tolerated prior to the load being scheduled.
- 6) Load departure time ($\tau_t^{j,i}$): The time slot at which the load departs after completing its operation.

Let $U_t^{j,i}$ be the number of unit energy packets $P_t^{j,i}$ demanded by a smart home j of load i at time slot t . The total energy packets required by all smart homes (M) with loads (N) during scheduling horizon (T_0) is computed by

$$P_{T_0}^{M,N} = \sum_{j=1}^M \sum_{i=1}^N \sum_{t=0}^{T_0-1} U_t^{j,i} \times P_t^{j,i}. \quad (1)$$

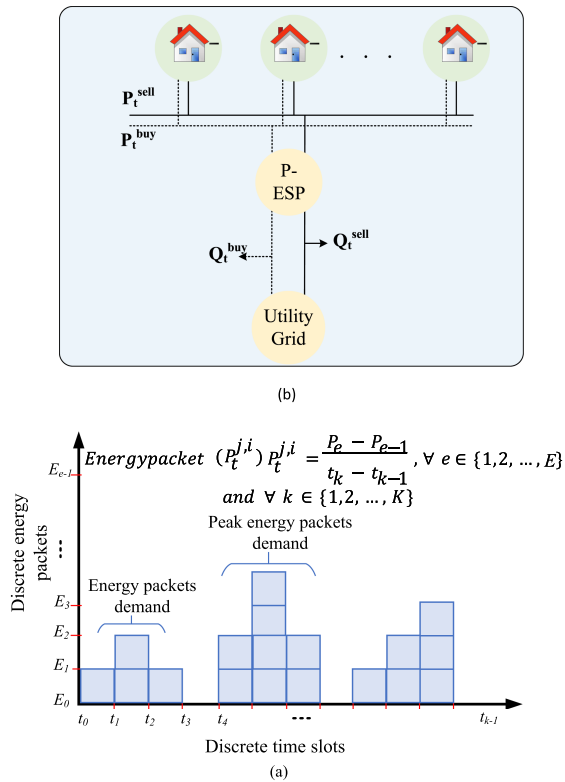


Fig. 2. Energy pricing under P-ESP. (a) Energy packet and (b) energy pricing model.

During appliance scheduling, the following user defined QoS constraint should be satisfied:

$$\varrho_t^{j,i} \leq \zeta_t^{j,i} + \rho_t^{j,i} \leq d_{t,\max}^{j,i}. \quad (2)$$

Equation (2) ensures that a given appliance i in a smart home j is scheduled at t without violating its delay requirement ($d_{t,\max}^{j,i}$), considering its arrival time ($\varrho_t^{j,i}$) and its length of operation time ($\zeta_t^{j,i}$). During the scheduling duration (T_0), appliances with $d_{t,\max}^{j,i} > 0$ can be delayed from their respective arrival times ($\varrho_t^{j,i}$'s), thereby adding flexibility to the load scheduling process. However, this flexibility (i.e., load scheduling delay) may adversely affect user comfort, if it goes beyond a specific user-defined level. Let $d_t^{j,i}$ be the delay experienced by load i in smart home j at t after serving [23], [27], such that

$$d_t^{j,i} = \frac{\zeta_t^{j,i} - \varrho_t^{j,i}}{d_{t,\max}^{j,i} - \zeta_t^{j,i}} \quad (3)$$

in which, if $\varrho_t^{j,i} = \zeta_t^{j,i}$ then $d_t^{j,i} = 0$, and the load is served immediately; otherwise, delay is incurred. A greater value of $d_t^{j,i}$ in (3) reflects the downgraded comfort level of the smart home user. Thus, (4) is modeled to impose user QoS-based lower and upper limits on d_t^i

$$d_{t,\min}^i \leq d_t^i \leq d_{t,\max}^i. \quad (4)$$

Using (5), the average delay incurred of any load i in a smart home j during T_0 is obtained as

$$\bar{d}_{T_0}^{M,N} = \frac{1}{M} \sum_{j=1}^M \sum_{t=0}^{T_0-1} \sum_{i=N}^M d_t^{j,i}. \quad (5)$$

Finally, (6) guarantees that the user QoS-based average bounds (0 and $\bar{d}_{T_0,\max}^{j,i}$) on $\bar{d}_{T_0}^{j,i}$ are satisfied during scheduling horizon T_0

$$0 \leq \bar{d}_{T_0}^{j,i} \leq \bar{d}_{T_0,\max}^{j,i}. \quad (6)$$

From the above analysis, it is clear that load scheduling, if allowed to operate under user QoS-based allowable delay bounds, adds flexibility to the scheduling process. However, this flexibility may have a counter-productive effect on user comfort if it goes beyond the user QoS-based specifications. Let $K_d(\bar{d}_{T_0}^{M,N})$

be a function to indicate the cost due to $\bar{d}_{T_0}^{j,i}$ based on the assumptions that $K_d(\cdot)$ is a nondecreasing continuous convex function and its derivative $K'_d(\cdot) < \infty$. Thus, here our objective is to minimize $K_d(\bar{d}_{T_0}^{M,N})$.

B. Energy Price Model

Smart homes, equipped with ERs and energy sources, are either having insufficient or adequate energy packets. Energy-insufficient smart homes have a greater energy demand than their locally generated and stored energy, and smart homes which possess adequate energy packets have a smaller energy demand than their locally generated and stored energy. Energy-deficient smart homes can buy energy packets ($H_t^{j,buy} = [H_{t,1}^{j,buy}, \dots, H_{t,i}^{j,buy}, \dots, H_{t,I}^{j,buy}]$) from an utility grid through a P-ESP to satisfy their demand. On the contrary, smart homes with excess energy packets can sell ($H_t^{j,sell} = [H_{t,1}^{j,sell}, \dots, H_{t,i}^{j,sell}, \dots, H_{t,I}^{j,sell}]$) back to the utility grid through the P-ESP. This process of energy packets exchange (buying and selling) is conducted by an energy pricing model of the P-ESP, which is formulated based on the constraints of feed-in-tariff of the utility, and demand-and-supply ratio (R_t^{DS}) within the energy packet sharing zone. The P-ESP acts as an agent for M smart home prosumers. It can buy energy packets from smart homes and the utility grid at unit prices $H_t^{j,buy}$ and J_t^{buy} , and sells energy packets to them at unit prices $H_t^{j,sell}$ and J_t^{sell} , respectively [24]. This can be formulated as

$$H_t^{j,sell} = \begin{cases} \frac{J_t^{sell} J_t^{buy}}{(J_t^{buy} - J_t^{sell}) R_t^{DS} + J_t^{sell}} & \text{if } 0 \leq R_t^{DS} \leq 1 \\ J_t^{sell} & \text{otherwise.} \end{cases} \quad (7)$$

It is noticed from (7) that:

- 1) if $R_t^{DS} = 0$, the smart home prosumers have insufficient energy packets to sell therefore, energy packets are bought from the utility at J_t^{buy} ;
- 2) if $R_t^{DS} \geq 1$, the smart home prosumer possess surplus energy packets which can be sold back to the utility grid at J_t^{sell} ;
- 3) if $0 < R_t^{DS} < 1$, the energy packets selling price is dynamically regulated between J_t^{sell} and J_t^{buy} .

Meanwhile, considering the energy packet selling cost, P-ESP's charge and utility's charge, an energy packet buying price is defined as

$$H_t^{j,buy} = \begin{cases} H_t^{j,sell} R_t^{DS} + J_t^{buy}(1 - R_t^{DS}) & \text{if } 0 \leq R_t^{DS} \leq 1 \\ J_t^{sell} & \text{otherwise} \end{cases} \quad (8)$$

where in (8), $0 < R_t^{DS} < 1$ shows that the overall energy packets demand are greater than the total energy packet supply of the smart home prosumers in the energy packet sharing zone, and this energy packet insufficiency is satisfied by procuring energy packets from the utility grid at J_t^{buy} . In-line with the above context, let $K_t^{j,buy}$ indicates the cost of energy packets bought by smart home j from the utility grid at time slot t via P-ESP

$$K_t^{j,buy} = H_t^{j,sell} \left(P_t^{M,L} - (E_{t,pv}^j + E_t^{j,s}) \right) \quad (9)$$

if $E_t^{M,L} > E_{t,pv}^j + E_t^{j,s}$

here in (9), $H_t^{j,sell}$ represents the selling cost of energy packets, $P_t^{M,L}$ is the total energy packets demands at time t , and $E_{t,pv}^j, E_t^{j,s}$ are available energy from rooftop PV and energy storage system at time instant j . It is also assumed that a smart home j buys energy packets only if the total energy packets demand can not be satisfied by $E_{t,pv}^j + E_t^{j,s}$. Similarly, (10) formulates the cost of energy packets sold by smart home j to the utility grid at time slot t via P-ESP

$$K_t^{j,sell} = H_t^{j,buy} \left((E_{t,pv}^j + E_t^{j,s}) - P_t^{M,L} \right) \quad (10)$$

if $E_{t,pv}^j + E_t^{j,s} > P_t^{M,L}$.

Further, the smart home users can sell the surplus energy packets given that $E_{t,pv}^j + E_t^{j,s}$ must be greater than demand of $P_t^{M,L}$. As per [25], eq. (9) and (10)] the average cost of the energy packets transaction (\bar{K}_t^{tx}) can be expressed as

$$\bar{K}_{T_0}^{M,tx} = \frac{1}{M} \sum_{t=0}^{T_0-1} \sum_{j=1}^M \left(K_t^{j,sell} - K_t^{j,buy} \right). \quad (11)$$

Here, the goal is to maximize the prosumer's energy packet revenue by minimizing the difference between $K_t^{j,sell}$ and $K_t^{j,buy}$. However, the process of energy packets buying and selling is constrained by the following:

$$\sum_{j=1}^M \sum_{i=1}^N \sum_{t=0}^{T_0-1} x_t^{j,i} = H_{T_0}^{M,L} \quad (12)$$

$$P_{t,\min}^{j,i} \leq x_t^{j,i} \leq P_{t,\max}^{j,i} \quad (13)$$

$$0 \leq H_t^{j,buy} \leq H_{t,\max}^{j,buy} \quad (14)$$

$$0 \leq H_t^{j,sell} \leq H_{t,\max}^{j,sell} \quad (15)$$

$$H_t^{j,i} - x_t^{j,i} \leq B_{\max} \quad (16)$$

where (12) implies that ERs can schedule the flexible loads in smart homes at other allowable time slots ($x_t^{j,i}$), while keeping the total energy packets demand constant. Likewise, (13) guarantees that the scheduling of flexible loads ($x_t^{j,i}$) must not

exceed smart home's base energy packet demand ($P_{t,\min}^{j,i}$) and the upper bound on supply capacity ($P_{t,\max}^{j,i}$). Constraints (14) and (15) ensure that energy procurement and selling criteria should be controlled and can not exceed given limits i.e., $H_{t,\max}^{j,buy}$ and $H_{t,\max}^{j,sell}$. Finally, (16) constraints on the feed-in energy packets when the utility grid restricts the selling of additionally generated energy packets (B_{\max}) due to grid security issues.

C. PV System

As mentioned earlier, roof-top PV panels are installed in the smart homes converting solar energy to electrical energy. Based on the model in [28], let $E_{t,pv}$ be the total amount of harvested energy from the PV panels by M smart homes over the entire horizon (T_0) such that

$$E_{T_0,pv}^M = \sum_{j=1}^M \sum_{t=0}^{T_0-1} E_{t,pv}^j \quad (17)$$

from (17), $E_{t,pv}$ can be calculated as $E_{t,pv} = \eta_{pv} \times A_{pv} \times I_{ir}(1 - 0.005(K_t((t) - 25)))$, the symbols η_{pv} , A_{pv} , and I_{ir} signify conversion efficiency, generator area, and solar irradiance, respectively. While 0.005 is the value use for temperature correction factor (TCF), and K_t represents outdoor temperature. Let $E_{t,pv}^c$ be the energy consumed from $E_{t,pv}$ in (18) with respective constraint (19) as given as follows:

$$E_{t,pv}^{c,j} = \min \left\{ x_t^{N,M}, E_{t,pv}^j \right\} \quad (18)$$

$$0 \leq E_{t,pv}^j \leq E_{t,pv}^j - E_{t,pv}^{c,j} \quad (19)$$

$$E_{t,pv}^j + E_t^g \in [0, \min\{S_{\max}, E_{t,\max}^{j,s} - E_t^{j,s}\}]. \quad (20)$$

From (18) and (19), it is clear that $E_{t,pv}^j$ is firstly supplied to the scheduled load in j at t ($x_t^{N,M} = \sum_{j=1}^M \sum_{i=1}^N x_t^{i,j}$), and the remaining part ($E_{t,pv}^r$), if any, is stored in an in-home energy storage system (according to (20)). It is worth noting that charging and discharging events of the battery cause a degradation cost in it. Hence, to manage charging or discharging events, PEM-ER can determine whether to store or not the conserved portion of $E_{t,pv}^j$ (i.e., $E_{t,pv}^{r,j}$) in the battery based on joint optimization.

D. Energy Storage System

During the time horizon T_0 the energy storage system can be operated by three possible states: 1) charging; 2) discharging; 3) idle considering the current energy packet demand and supply conditions. That is, during charging state, it can either be charged from the PV panels, the P-ESP, or a combination of both. Likewise, during discharging state, it can be discharged to satisfy the energy packet need of various loads. In an idle state, it is neither charging nor discharging. These state transitions are bounded by the following:

$$k_t^j \in [0, \min\{k_{\max}^j, E_t^{j,s} - E_{t,\min}^{j,s}\}] \quad (21)$$

$$0 \leq E_{t,pv}^j + E_t^g \leq S_{\max} \quad (22)$$

$$0 \leq k_t^j \leq k_{\max}^j \quad (23)$$

$$E_{t,\min}^{j,s} \leq E_t^{j,s} \leq E_{t,\max}^{j,s}. \quad (24)$$

Specifically, (21) and (22) imply that charging and discharging demand at time t can be met by the available energy in the battery. (22) also limits that the total charging amount ($E_{t,pv}^j + E_t^g$) at time slot t does not exceed its upper limit (S_{\max}), while (23) restricts the total discharging amount in j at t (k_t^j) by its upper bound (k_{\max}^j). Equation (24) imposes per slot minimum and maximum capacity constraints ($E_{t,\min}^{j,s}$ and $E_{t,\max}^{j,s}$) on the current energy state of the battery ($E_t^{j,s}$). The current energy state of the battery system is computed as

$$E_{t+1}^{j,s} = \alpha_t E_t^{j,s} + \eta_t^{(+)} (E_{t,pv}^j + E_t^g) - \eta_t^{(-)} (k_t^j) \quad (25)$$

in (25) α_t , $\eta_t^{(+)}$, and $\eta_t^{(-)}$ signify decay rate in the battery, the efficiencies of charging and discharging activities, respectively.

Let $a_t^{(+)} \triangleq \{1, \text{if } E_{t,pv}^j + E_t^g > 0; 0, \text{otherwise}\}$ specify whether an event charging occurred ($a_t^{(+)} = 1$) or not ($a_t^{(+)} = 0$). Likewise, $a_t^{(-)} \triangleq \{1, \text{if } k_t^j > 0; 0, \text{otherwise}\}$ is considered for a discharging event. In this regard, charging and discharging events lead to degradation cost in the battery, indicated by $c_t^{(+)}$ and $c_t^{(-)}$, respectively. Based on a thorough analysis in [29], [30], [31], [32], and [33], the battery degradation costs at t can be formulated as follows:

$$c_t^{j,(+)} = \frac{h_r}{h_t} \left\{ \left(\frac{E_{pv}^{r,j} + E_t^g}{E_{t,pv}^j + E_t^g} \right)^{w_0} \times \exp^{w_1 \left(\frac{E_{t,pv}^j + E_t^g}{E_{pv}^{r,j} + E_t^g} - 1 \right)} \right\} \quad (26)$$

$$c_t^{j,(-)} = \frac{h_r}{h_t} \left\{ \left(\frac{k_r}{k_t^j} \right)^{w_2} \times \exp^{w_3 \left(\frac{k_t^j}{k_r} - 1 \right)} \right\}. \quad (27)$$

In (26) and (27), $c_t^{j,(+)}$, $c_t^{j,(-)}$ represent battery degradation cost occur due to its charging and discharging activities in a smart home j . It can be noted that the lifetime of the battery storage system depends on fast variation of charging (i.e., $E_{t,pv}^j + E_t^g$) and discharging (k_t^j) activities, however, if charging and discharging are kept at their rated values then the lifetime of the storage battery is affected by current variations corresponding to their rated values. Therefore, based on (26) and (27), the degradation cost of a the battery in a smart home j at t is given in the following, its average is computed over T_0 as:

$$K_t^{j,s} = a_t^{(+)} c_t^{j,(+)} + a_t^{(-)} c_t^{j,(-)}, \quad a_t^{(+)} + a_t^{(-)} \leq 1 \quad (28)$$

$$\overline{K}_{T_0}^{M,s} = \frac{1}{M} \sum_{j=1}^M \sum_{t=0}^{T_0-1} K_t^{j,s}. \quad (29)$$

The objective here is to minimize the average battery degradation cost in (29).

From the above discussions, it is clear that minimizing (30) is a joint stochastic optimization problem between the three considered system costs. And solving this problem through traditional mathematical optimization techniques is computationally expensive and required high assessment [16], [17], [18]. Therefore, in the next section, heuristic optimization techniques are adopted to solve the joint stochastic optimization problem of (30).

III. PROBLEM FORMULATION

Let $\theta_t \triangleq [E_t^g, E_{t,pv}^c, E_{t,pv}^r, k_t^j]$ be an energy flow vector and control actions for smart homes at time slot t . The aim here is to minimize an average aggregated system cost which consists of the following parts:

- 1) the energy packet transactions cost (selling and buying) with the P-ESP ($\overline{K}_{T_0}^{M,tx}$);
- 2) household load scheduling delays cost ($K_d(\overline{d}_{T_0}^{M,N})$);
- 3) energy storage battery degradation cost ($\overline{K}_{T_0}^{M,s}$).

Our aim is to find an optimal policy $\{\theta_{T_0}, d_{T_0}^{M,N}\}$, while minimizing the average system cost. Thus, the problem can be formulated as

$$\text{minimize: } K_d(\overline{d}_{T_0}^{M,N}) + \overline{K}_{T_0}^{M,tx} + \overline{K}_{T_0}^{M,s} \quad (30)$$

$$\{\theta_{T_0}, d_{T_0}^{M,N}\}$$

where $d_t^{j,i} \triangleq [d_t^{1,1}, d_t^{2,2}, \dots, d_t^{M,N}]$, and $K_d(\overline{d}_{T_0}^{M,N}) \triangleq [K_d(\overline{d}_{T_0}^{1,1}), K_d(\overline{d}_{T_0}^{2,2}), \dots, K_d(\overline{d}_{T_0}^{M,N})]$. The cost function in (30) and the formulated constraints in (6)–(24) are related to energy scheduling, energy procurement, and energy control as discussed in the previous Sections II-A and II-D. Clearly, the optimization problem in (30) is a joint stochastic optimization problem between the three considered system costs. This joint scheduling makes the problem difficult to solve by traditional mathematical optimization techniques [12], [13], [14]. Therefore, in the next section, heuristic optimization techniques are adopted to solve the joint stochastic optimization problem of (30).

IV. OPTIMIZATION TECHNIQUES

Heuristic optimization techniques are generally employed to solve scheduling problems due to their ability to solve high dimensional and complex problems with fast convergence, ease in implementation, and local optima avoidance capabilities [20], [21], [22], [23]. Thus, we employ the following well-known heuristic algorithms: GA, BPSO [34], DE, and HSA [35] methods. These algorithms are briefly discussed in the following.

A. Genetic Algorithm

The GA [35] is employed to solve the joint optimization problem in (30) through the following steps.

1) Population generation: Initialize a set of random population (P_0) such that $X_a \in \{1 \text{ if } P_0(a) > 0.5, \text{otherwise } 0\}$. The individuals in P_0 are binary coded X_{ab} , $b \in [1, k]$ where k is a dimensional vector denoting the operation of load as ON and OFF states. The algorithm parameters; P_0 , crossover, mutation types (C_{bt} , M_{bt}), and probabilities (P_c , P_m), respectively, where bt is the set of positive integers.

2) System inputs: Obtain the input values of $P_{T_0}^{M,L}$, $d_t^{j,i}$, E_t^g , $E_{t,pv}^j$, $E_t^{j,s}$, P_t and set upper and lower bounds according to Section II.

3) Evaluation: Calculate $K_d(\overline{d}_{T_0}^{M,N})$, $\overline{K}_{T_0}^{M,tx}$, and $\overline{K}_{T_0}^{M,s}$ with the given constraints (2), (4), (6)–(10), (13), (16), (18)–(24).

4) Updating P_0 : The set of individuals in P_0 are modified and go through crossover and mutation with a probability range between 0 and 1. In each iteration, *stochastic operators* are applied (until *generations* reach a preset number) to achieve optimal solutions and minimize (30).

B. Binary Particle Swarm Optimization

The joint optimization problem in (30) is solved via the BPSO [35] algorithm through the following steps.

1) Population generation: Initialize the swarm (S_0) in a pair $(\overrightarrow{ps}_r, \overrightarrow{v}_r)$ using (31). The algorithm parameters are set, including maximum and minimum velocities of the particles, normal distribution between 0 and 1. The position ps_r of the particle r is computed as

$$\overrightarrow{ps}_r(t) = \overrightarrow{ps}_r(t-1) + \overrightarrow{v}_r(t) \quad (31)$$

where $\overrightarrow{ps}_r, \overrightarrow{v}_r \in \mathbb{R}^n$ represent position and velocity of the particles and $\overrightarrow{ps}_r(t-1)$ is the prior position of the particle in S_0 .

2) System inputs: Obtain the required input values as mentioned in Section IV-A with upper and lower bounds according to Section II.

3) Evaluation: Calculate $K_d(\overrightarrow{d}_{T_0}^{M,N})$, $\overline{K}_{T_0}^{M,tx}$, and $\overline{K}_{T_0}^{M,s}$ with the given constraints (2), (4), (6)–(10), (13), (16), (18)–(24). The particles in this evaluation are named as p_{best} .

4) Updating S_0 : For the optimal values of S_0 , the search space is refined/alterd according to

$$\begin{aligned} \overrightarrow{v}_r(t) = & \overrightarrow{v}_r(t-1) + \alpha_1 \text{rand}_1(p_r - \overrightarrow{ps}_r(t-1)) + \dots \\ & \alpha_2 \text{rand}_2(p_g - \overrightarrow{ps}_r(t-1)) \end{aligned} \quad (32)$$

$$\overrightarrow{v}_r(t) = \begin{cases} \overrightarrow{v}_r^{\max} & \text{if } \overrightarrow{v}_r > \overrightarrow{v}_r^{\max} \\ \overrightarrow{v}_r^{\min} & \text{if } \overrightarrow{v}_r < \overrightarrow{v}_r^{\min} \end{cases} \quad (33)$$

where $\alpha_1 \cdot \text{rand}_1$ and $\alpha_2 \cdot \text{rand}_2$ are random weights for p_r (local) and p_g (global) positions of the particles, respectively. In (33) $\overrightarrow{v}_r^{\max}$ and $\overrightarrow{v}_r^{\min}$ signify the maximum and minimum velocities of particle r at random point, respectively. It is to be observed that \overrightarrow{ps}_r is constrained between [0, 1]. The updated particles in S_0 are further tested in the *evaluation* step to achieve best values (until *generations* reach a preset number).

C. Differential Evolution Algorithm

The joint optimization problem in (30) is solved through the DE algorithm [36] involving the steps given below.

1) Population generation: Initial population $P_1 \in \mathbb{R}^n$ is obtained from (34) with p_e^U, p_e^L being the upper and lower bounds of P_1 , respectively, where rand_i is a uniformly distributed random number between 0 and 1.

$$P_1 = p_e^L + \text{rand}_i(p_e^U - p_e^L). \quad (34)$$

2) System inputs: Obtain the required input values as mentioned in Section IV-A with upper and lower bounds according to Section II.

3) Evaluation: Calculate $K_d(\overrightarrow{d}_{T_0}^{M,N})$, $\overline{K}_{T_0}^{M,tx}$, and $\overline{K}_{T_0}^{M,s}$ while respecting the constraints given in (2), (4), (6)–(10), (13), (16), and (18)–(24).

4) Updating P_1 : P_1 is updated through mutation process using (35) and new trial vector T_v is obtained by crossover using (36)

$$\begin{aligned} M_{de} &= v_{r1} + F(v_{r2} - v_{r3}) \quad (35) \\ T_v &= \begin{cases} M_{de} & \text{if } \text{rand}(j) \leq cr \\ P_1 & \text{if } \text{rand}(j) > cr \end{cases} \quad (36) \end{aligned}$$

where F in (35) is a constant between [0, 1], v_{r1}, v_{r2} , and v_{r3} are the vectors (randomly) chosen from P_1 and $r1, r2, r3$ are positive integers $\in \{1, 2, 3, 4, \dots, n\}$. Through crossover (cr), new trial vector is generated as per (36). The updated individuals in P_1 are further tested in the *evaluation* step to achieve the best individuals until *generation* reaches a preset number.

D. Harmony Search Algorithm

The joint optimization problem in (30) is solved through the HSA algorithm [35] implemented via the following steps.

1) Population generation: Initialize harmony memory (HM) size and other parameters of the algorithm; such as HM consideration rate (HM_c), pitch adjustment ratio (Pa), minimum and maximum bandwidth (b_{\min}, b_{\max})

2) Inputs: Obtain the required input values as mentioned in Section IV-A with upper and lower bounds according to Section II.

3) Evaluation: Calculate $K_d(\overrightarrow{d}_{T_0}^{M,N})$, $\overline{K}_{T_0}^{M,tx}$, and $\overline{K}_{T_0}^{M,s}$ while respecting the constraints given in (2), (4), (6)–(10), (13), (16), and (18)–(24).

4) Updating HM size: The individuals in HM are updated based on (37). The new harmony is further diversified using Pa as per (38)

$$HM = \begin{cases} HM \in HM_{old} & \text{with } P(HM_c) \\ HM \in HM_{new} & \text{with } P(HM_c - 1) \end{cases} \quad (37)$$

$$HM = \begin{cases} Yes & \text{with } P(Pa) \\ No & \text{with } P(1 - Pa). \end{cases} \quad (38)$$

In each iteration, HSA operators $P(HM_c)$ and $P(Pa)$ are applied to HM to strive for optimal solutions until *generations* reach a preset number.

V. RESULTS AND DISCUSSION

In this section, we present simulation results of the designed ER-PEM system model based on the selected four HOMs: GA, BPSO, DE, and HSA. We benchmark the performance of HOMs based on energy scheduling parameters (i.e., energy balance, average transactions, average delay, and average system cost) in varying seasons and under different values of HOMs' hyperparameters.

For simulations purpose, we assume $M = 10$ smart homes with the same energy profiles for a finite scheduling horizon of 24 hours (starting from 1:00 A.M. to the next day at 1 A.M.) [37]. Further, PV energy is generated randomly varying over T_0 and I_{ir} with $\overline{E}_{t,pv}^{\max} = 8$ kWh for summer season, $\overline{E}_{t,pv}^{\max} = 5$ kWh for spring season, and $\overline{E}_{t,pv}^{\max} = 3$ kWh for winter with $\eta_{pv} = 18\%$. An energy storage system of $\overline{E}_{t,max}^s = 5$ kWh with $\alpha_t = 0.8$ and $\eta_t^{(+)} = \eta_t^{(-)} = 0.7$ is considered. Data related to

TABLE II
SELECTED VALUES OF HYPERPARAMETERS

HOMs	Hyper-parameters				
		Selection I	Selection II	Selection III	Selection IV
GA	C_{bt}	1	2	3	4
	M_{bt}	1	2	3	4
	P_c, P_m	[0.9, 0.1]	[0.8, 0.2]	[0.7, 0.5]	[0.5, 0.4]
BPSO	$\vec{v}_r^{\max}, \vec{v}_r^{\min}$	[4, -4]	[6, -6]	[8, -8]	[10, -10]
	$\alpha_1 = \alpha_2$	1	3	3	5
	\vec{v}_r	2	3	4	8
DE	F	0.7	0.8	0.9	0.5
	P_{ce}	0.9	0.8	0.7	0.5
	$p_e^{L,u}$	[30, 100]	[60, 150]	[70, 200]	[100, 300]
HSA	HMc	0.9	0.8	0.7	0.5
	$Pa_{\min, \max}$	[0.01, 1]	[0.05, 1]	[0.5, 1]	[0.05, 1]
	$b_{\min, \max}$	[0.001, 1]	[0.002, 1]	[0.004, 1]	[0.02, 1]

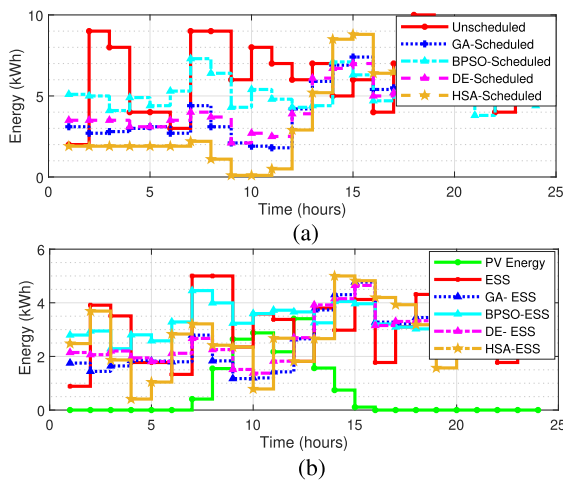


Fig. 3. Unscheduled case versus selected optimization algorithms. (a) Demand and supply balance and (b) energy storage system balance.

solar irradiance and temperature is obtained from the Finnish Meteorological Institute (FMI) [38]. We consider that smart home users can buy or sell their energy packets from or to the utility with $H_{t, \min}^{buy} = 0.6$ cents/kWh, $H_{t, \max}^{buy} = 3.7$ cents/kWh, $H_{t, \min}^{sell} = 0.06$ cents/kWh and $H_{t, \max}^{sell} = 0.57$ cents/kWh [39]. We also consider following sets of hyperparameters:

- 1) selection of C_{bt}, M_{bt}, P_c, P_m for GA;
- 2) selection of $\vec{v}_i^{\max}, \vec{v}_i^{\min}, \alpha_1, \alpha_2, \vec{v}_i$ for BPSO;
- 3) selection of F, P_{ce}, p_e^L, p_e^u for DE;
- 4) selection of $HMc, Pa_{\min}, Pa_{\max}, b_{\min}, b_{\max}$ for HSA.

The HOMs are analyzed under varied selection sets of their respective values of hyperparameters as given in Table II. We run our simulation using MATLAB scripts (version R2018b) on a 2.5-GHz PC with 32 GB RAM.

Fig. 3 shows energy balance results for the unscheduled case against the selected HOMs (i.e., GA, BPSO, DE, and HSA). It is clear from Fig. 3 that energy demand of smart homes is met from the on-site renewable resources and external power grid. It can be seen from Fig. 3 that PV energy is insufficient to meet the energy demand of smart homes, however, it is used efficiently by HOMs. Whenever possible, the smart homes procure energy at low prices from the utility grid to meet their energy demand. It

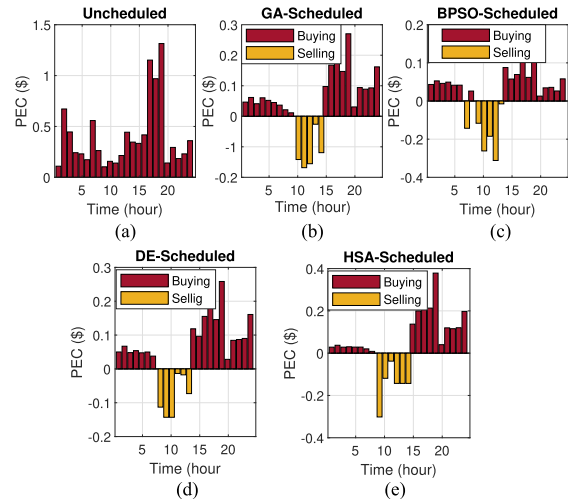


Fig. 4. Average energy transactions between users and P-ESP.

can be further noted from Fig. 3 that the selected HOMs schedule the demand of smart homes efficiently while respecting system constraints as discussed in Sections II and III.

Fig. 4 depicts relative performance of the selected HOMs against the unscheduled case in terms of the PEC involving selling of energy packets to and buying of energy packets from the P-ESP over T_0 . In the unscheduled case [see Fig. 4(a)], energy packet transactions are unidirectional only, i.e., E_t 's are bought by smart home customers at 2.30\$/for $E_{t, \max}$. By contrast, the heuristic algorithms [see Fig. 4(b)–(e)] carry bidirectional energy packet transactions among smart home customers and the P-ESP. Fig 4 reflects that the HOMs are efficient to balance the energy demand of smart homes as well as empower the smart home customers to sell surplus energy. Particularly, smart home customers buy energy during 1–5 A.M. When the available PV generated energy exceeds the demand during day time, the surplus energy packets are sold back to the P-ESP.

Quantitatively, the selling costs (in \$/slot) for GA, BPSO, DE, and HSA algorithms are 0.61, 1.04, 0.51, and 0.89, respectively. The performance comparison of algorithms shows that the BPSO and HSA utilize the harvested energy from the PV system and energy storage system in a more efficient manner than the GA, and the DE—selling greater amount of energy packets to the P-ESP. This validates that the heuristic optimization algorithms allocate energy resources effectively and facilitate customers to sell back their surplus energy to the utility grid via the P-ESP. Table III illustrates the buying and selling cost of the M smart homes on daily and monthly basis. As mentioned previously, in an unscheduled case, the energy packet transactions are unidirectional and the daily average buying cost is 1.9 \$. By contrast, with the inclusion of HOMs, smart home customers are able to sell the surplus energy at an average cost of 0.61, 1.04, 0.51, and 0.89 \$ by the GA, BPSO, DE, and HSA, respectively, as shown in Table III. It can be observed from the table that the selling cost of energy packets under various hyperparameters' selection remains constant except for selection IV, where the cost slightly increases by 0.11 (\$/slot) for GA, DE, HSA, and 0.6 (\$/slot) for BPSO. On the other hand, the procurement cost

TABLE III
AVERAGE ENERGY TRANSACTIONS BETWEEN SMART HOMES AND P-ESP

HOMs	Hyperparameters' selection	P-ESP Energy (buy) (\$)	P-ESP Energy (sell) (\$)	Daily bill (\$)	Monthly bill (\$)
Unscheduled	–	1.90	–	1.90	57
GA-Scheduled	I	1.79	0.61	1.18	35.4
	II	1.46	0.61	0.85	25.5
	III	1.55	0.61	0.94	28.2
	IV	1.62	0.72	0.90	27
BPSO-Scheduled	I	1.85	1.04	0.81	24.3
	II	1.53	1.13	0.40	12
	III	1.49	1.13	0.36	10.8
	IV	1.46	1.19	0.27	8.1
DE-Scheduled	I	1.83	0.51	1.32	39.6
	II	1.62	0.51	1.11	33.3
	III	1.65	0.51	1.14	34.2
	IV	1.63	0.61	1.02	30.6
HSA-Scheduled	I	1.99	0.89	1.1	33
	II	1.69	0.89	0.8	24
	III	1.66	0.89	0.77	23.1
	IV	1.64	0.91	0.73	21.9

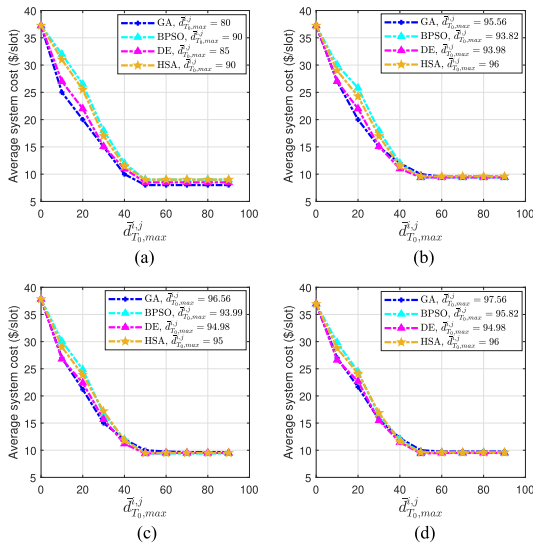


Fig. 5. Performance of HOMs under the hyperparameters' selection I–IV (a)–(d): average system cost vs $\bar{d}_{T_0,\max}^{j,i} \forall i, j \in [N, M]$.

of energy packets varies with the selection of different values of hyperparameters. Essentially, the inclusion of hyperparameters' selection (I–IV) reflects that HOMs has improved the scheduling process (by selling the energy packets and procuring energy packets at low prices) and reduced the overall PEC of smart home customers.

Fig. 5(a)–(d) show the impact of load scheduling delay of the selected algorithms on the average system cost under the hyperparameters' selection I–IV. The average system cost is calculated as energy procurement cost, scheduling delay cost, and battery degradation cost (as mentioned in Section III). The average system cost can be increased/decreased based on the allowable load scheduling delays, which means relaxing the allowable delay can decrease the average cost of the system and vice versa. This relation is depicted in Fig. 5 as strict scheduling delay of the algorithms results in higher average system cost, whereas when scheduling delay is allowed to relax,

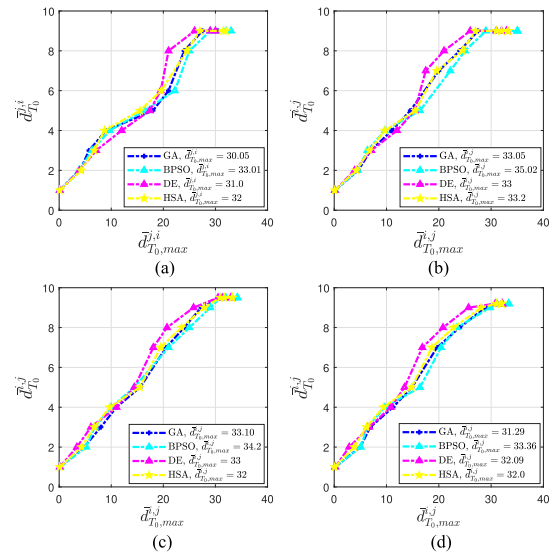
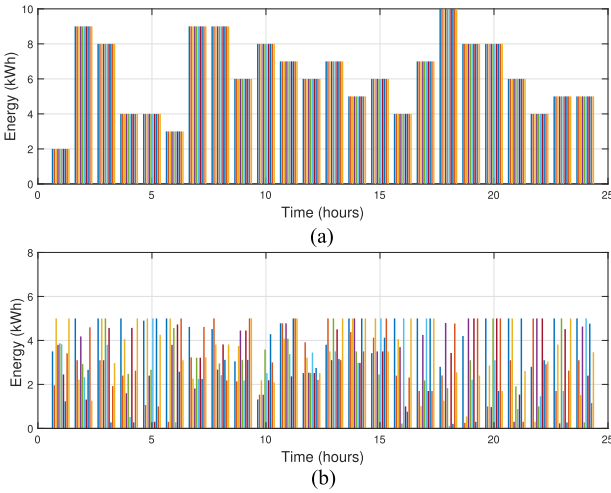


Fig. 6. Delay performance of HOMs under the hyperparameters' selection I–IV (a)–(d): $\bar{d}_{T_0}^{j,i}$ vs $\bar{d}_{T_0,\max}^{j,i} \forall i, j \in [N, M]$.

the cost of the system is reduced. It is important to note that this tradeoff can help the users to operate scheduling delays at their desired level with respect to the average cost of the system. Similarly, the impact of the hyperparameters' selections (II, III, IV) for the average system cost versus $\bar{d}_{T_0,\max}^{j,i}$ is also shown in Fig. 5(b)–(d). It is evident from Fig. 5(a)–(d) that HOMs follow similar behavior, however, the gap between the performance curves of HOMs is decreasing. Essentially, this means that selection of different hyperparameter values improves the randomization process of HOMs and provides effective solutions to the optimization problems. Fig. 6(a)–(d) depict a performance comparison of $\bar{d}_{T_0}^{j,i}$ vs $\bar{d}_{T_0,\max}^{j,i}$ between HOMs (GA, BPSO, DE, and HSA) based on the hyperparameter selection I–IV. It can be observed in Fig. 6 that average experienced delay $\bar{d}_{T_0}^{j,i}$ by load i in a smart home j increases when the $\bar{d}_{T_0,\max}^{j,i}$ (maximum allowable delay requirement) is relaxed.

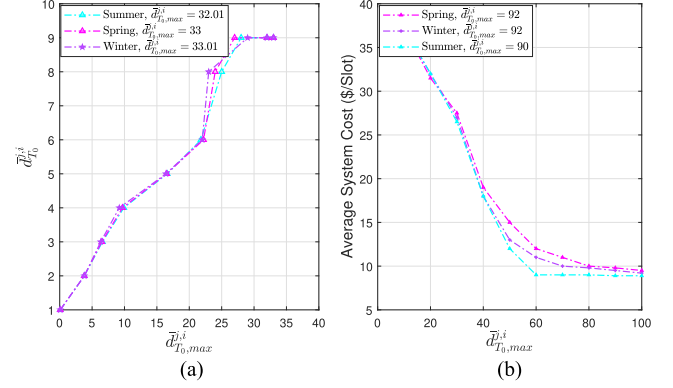
TABLE IV
 DELAY PERFORMANCE OF THE HOMs

Hyper-parameters	Performance of HOMs against $\bar{d}_{T_0}^{j,i}$ vs $\bar{d}_{T_0,max}^{j,i} \forall i, j \in [N, M]$
Selection I	BPSO, $\bar{d}_{T_0,max}^{j,i}=33.10$, HSA, $\bar{d}_{T_0,max}^{j,i}=32$, GA, $\bar{d}_{T_0,max}^{j,i}=30.05$, DE $\bar{d}_{T_0,max}^{j,i}=31$,
Selection II	BPSO, $\bar{d}_{T_0,max}^{j,i}=35.02$, GA, $\bar{d}_{T_0,max}^{j,i}=33.05$, HSA, $\bar{d}_{T_0,max}^{j,i}=33.2$, DE, $\bar{d}_{T_0,max}^{j,i}=33$,
Selection III	BPSO, $\bar{d}_{T_0,max}^{j,i}=34.2$, GA, $\bar{d}_{T_0,max}^{j,i}=33.10$, DE $\bar{d}_{T_0,max}^{j,i}=33$, HSA, $\bar{d}_{T_0,max}^{j,i}=32$
Selection IV	BPSO, $\bar{d}_{T_0,max}^{j,i}=33.36$, DE $\bar{d}_{T_0,max}^{j,i}=32.09$, HSA, $\bar{d}_{T_0,max}^{j,i}=32$ GA, $\bar{d}_{T_0,max}^{j,i}=31.29$


 Fig. 7. PEM plans for M smart homes. (a) Unscheduled and (b) BPSO-scheduled.

This behavior of $\bar{d}_{T_0}^{j,i}$ against $\bar{d}_{T_0,max}^{j,i}$ shows sublinear relation for the given algorithms. This means during scheduling process, the operation of the load i can be delayed to obtain flexibility in the average system cost, however, on the other hand, QoS would be compromised. It can also be observed from Fig. 6(a)–(d) that during the scheduling process, BPSO attains $\bar{d}_{T_0,max}^{j,i}$ and compromises QoS most in comparison to other algorithms which in turn reduces system cost. Note that, in Fig (a)–(c) the HOMs exhibit the same behavior (sublinear), however, the order of the algorithms in terms of $\bar{d}_{T_0,max}^{j,i}$ has changed due to different set of hyperparameters selection. This reflects that different values of hyperparameters can add flexibility to the scheduling process considering constraints of the scheduling parameters. The order of the algorithms in terms of $\bar{d}_{T_0,max}^{j,i}$ is presented in the Table IV.

It is worth mentioning that the ER-PEM provides the optimal energy plans for a single home, like HEMS and multiple homes considering the energy-demand requirement as discussed in Section II. Thus, for the sake of simplicity, here, we show the BPSO algorithm to demonstrate the PEM planes for 10 smart homes separately in Fig. 7. Fig. 7(a) and (b) represents the PEM plans for ten smart homes at “ t ” for an unscheduled case and the


 Fig. 8. Performance of the BPSO in different seasons condition. (a) $\bar{d}_{T_0}^{j,i}$ vs $\bar{d}_{T_0,max}^{j,i}$. (b) Average system cost versus $\bar{d}_{T_0,max}^{j,i} \forall i, j \in [N, M]$.

BPSO algorithm. It can be observed from Fig. 7(a) that the PEM plans without scheduling are uniform values for smart homes during “ t ” which consequently generates power peaks in peak hours. In contrast, Fig. 7(b) depicts that the algorithm BPSO tends to provide diverse PEM plans for each smart home in time slot “ t ” and avoids the peak consumption of energy. Fig. 8(a) and (b) shows the performance of the BPSO algorithm for T_0 during three days: summer–spring–winter in terms of the maximum allowable delay and the average cost of the system. In Fig. 8(a), when the season conditions varied from summer–spring–winter, the value of $\bar{d}_{T_0}^{j,i}$ increases reflecting demanding constraints of energy storage systems due to the increase in imbalance between R_t^{DS} . Next, Fig. 8(b) represents the effect of $\bar{d}_{T_0,max}^{j,i}$ on the average system cost considering varied season conditions. The tradeoff relation between the average system cost and $\bar{d}_{T_0,max}^{j,i}$ can be seen, which represents the average system cost can be lowered with the stringent load scheduling delay and vice versa.

VI. CONCLUSION

This article presents an ER-based PEM system for MAs in smart homes in the EI. The goal is to minimize the average aggregated system cost which consists of load scheduling delay cost, energy procurement cost, and battery degradation cost. To achieve the objective, we jointly optimize the energy usage of smart homes, grid-connected PV energy, and energy storage system. The ER-PEM solves the joint optimization problem considering the four well-known HOMs: GA, BPSO, DE, and HSA. Through simulations, the selected HOMs are benchmarked in terms of energy scheduling parameters, energy scheduling delays, energy balance, and average system cost parameters. Moreover, the performance of the ER-PEM is also evaluated by considering the impact of the hyperparameters of heuristic techniques and varying weather conditions on ER-PEM system. The results show that the ER-based PEM minimizes the average aggregated system cost and provides effective energy plans for a single smart home and in an energy community of multiple smart homes and varied season conditions. In the future, we aim to investigate the impact of electric vehicles integration on the EI under the assumptions of the proposed model.

REFERENCES

- [1] A. Ali, K. Mahmoud, and M. Lehtonen, "Optimization of photovoltaic and wind generation systems for autonomous microgrids with PEV-parking lots," *IEEE Syst. J.*, vol. 16, no. 2, pp. 3260–3271, Jun. 2022.
- [2] S. F. Santos, M. Gough, D. Z. Fitiwi, A. F. Silva, M. Shafie-Khah, and J. P. Catalão, "Influence of battery energy storage systems on transmission grid operation with a significant share of variable renewable energy sources," *IEEE Syst. J.*, vol. 16, no. 1, pp. 1508–1519, Mar. 2022.
- [3] J. Wang, J. Wei, Y. Zhu, and X. Wang, "The reliability and operational test system of a power grid with large-scale renewable integration," *CSEE J. Power Energy Syst.*, vol. 6, no. 3, pp. 704–711, 2019.
- [4] A. Perera, Z. Wang, V. M. Nik, and J.-L. Scartezzini, "Towards realization of an energy internet: Designing distributed energy systems using game-theoretic approach," *Appl. Energy*, vol. 283, 2021, Art. no. 116349.
- [5] K. Wang et al., "A survey on energy internet: Architecture, approach, and emerging technologies," *IEEE Syst. J.*, vol. 12, no. 3, pp. 2403–2416, Sep. 2018.
- [6] P. H. Nardelli et al., "Energy internet via packetized management: Enabling technologies and deployment challenges," *IEEE Access*, vol. 7, pp. 16909–16924, 2019.
- [7] M. Gao, K. Wang, and L. He, "Probabilistic model checking and scheduling implementation of an energy router system in energy internet for green cities," *IEEE Trans. Ind. Inform.*, vol. 14, no. 4, pp. 1501–1510, Apr. 2018.
- [8] P. Nardelli, H. M. Hussain, A. Narayanan, and Y. Yang, "Virtual microgrid management via software-defined energy network for electricity sharing: Benefits and challenges," *IEEE Syst., Man, Cybern. Mag.*, vol. 7, no. 3, pp. 10–19, Jul. 2021.
- [9] H. Guo, F. Wang, L. Zhang, and J. Luo, "A hierarchical optimization strategy of the energy router-based energy internet," *IEEE Trans. Power Syst.*, vol. 34, no. 6, pp. 4177–4185, Nov. 2019.
- [10] E. H. Et-Tolba, M. Maaroufi, and M. Ouassaid, "Demand side management in smart grid by multi-agent systems technology," in *Proc. Int. Conf. Multimedia Comput. Syst.*, 2014, pp. 1042–1045.
- [11] M. de Castro Tomé, P. H. Nardelli, H. M. Hussain, S. Wahid, and A. Narayanan, "A cyber-physical residential energy management system via virtualized packets," *Energies*, vol. 13, no. 3, 2020, Art. no. 699.
- [12] L. A. D. Espinosa and M. Almassalkhi, "A packetized energy management macromodel with quality of service guarantees for demand-side resources," *IEEE Trans. Power Syst.*, vol. 35, no. 5, pp. 3660–3670, Sep. 2020.
- [13] C. Tu, F. Xiao, Z. Lan, Q. Guo, and Z. Shuai, "Analysis and control of a novel modular-based energy router for DC microgrid cluster," *IEEE Trans. Emerg. Sel. Topics Power Electron.*, vol. 7, no. 1, pp. 331–342, Mar. 2019.
- [14] P. Li, W. Sheng, Q. Duan, Z. Li, C. Zhu, and X. Zhang, "A Lyapunov optimization-based energy management strategy for energy hub with energy router," *IEEE Trans. Smart Grid*, vol. 11, no. 6, pp. 4860–4870, Nov. 2020.
- [15] M. Rastegar, M. Fotuhi-Firuzabad, H. Zareipour, and M. Moeini-Aghaieh, "A probabilistic energy management scheme for renewable-based residential energy hubs," *IEEE Trans. Smart Grid*, vol. 8, no. 5, pp. 2217–2227, Sep. 2017.
- [16] J. A. A. Silva, J. C. López, N. B. Arias, M. J. Rider, and L. C. da Silva, "An optimal stochastic energy management system for resilient microgrids," *Appl. Energy*, vol. 300, 2021, Art. no. 117435.
- [17] M. Roslan, M. Hannan, P. J. Ker, R. Begum, T. I. Mahlia, and Z. Dong, "Scheduling controller for microgrids energy management system using optimization algorithm in achieving cost saving and emission reduction," *Appl. Energy*, vol. 292, 2021, Art. no. 116883.
- [18] A. Ahmad and J. Y. Khan, "Real-time load scheduling and storage management for solar powered network connected EVs," *IEEE Trans. Sustain. Energy*, vol. 11, no. 3, pp. 1220–1235, Jul. 2020.
- [19] R. Carli, M. Dotoli, J. Jantzen, M. Kristensen, and S. B. Othman, "Energy scheduling of a smart microgrid with shared photovoltaic panels and storage: The case of the Ballen Marina in Samsø," *Energy*, vol. 198, 2020, Art. no. 117188.
- [20] H. T. Dinh, J. Yun, D. M. Kim, K.-H. Lee, and D. Kim, "A home energy management system with renewable energy and energy storage utilizing main grid and electricity selling," *IEEE Access*, vol. 8, pp. 49436–49450, 2020.
- [21] D. Li, W.-Y. Chiu, H. Sun, and H. V. Poor, "Multiobjective optimization for demand side management program in smart grid," *IEEE Trans. Ind. Inform.*, vol. 14, no. 4, pp. 1482–1490, Apr. 2018.
- [22] F. Luo, W. Kong, G. Ranzi, and Z. Y. Dong, "Optimal home energy management system with demand charge tariff and appliance operational dependencies," *IEEE Trans. Smart Grid*, vol. 11, no. 1, pp. 4–14, Jan. 2020.
- [23] H. M. Hussain, N. Javaid, S. Iqbal, Q. U. Hasan, K. Aurangzeb, and M. Alhussein, "An efficient demand side management system with a new optimized home energy management controller in smart grid," *Energies*, vol. 11, no. 1, 2018, Art. no. 190.
- [24] J. S. Vardakas, N. Zorba, and C. V. Verikoukis, "A survey on demand response programs in smart grids: Pricing methods and optimization algorithms," *IEEE Commun. Surv. Tut.*, vol. 17, no. 1, pp. 152–178, Jan.–Mar. 2015.
- [25] L. Park, Y. Jang, S. Cho, and J. Kim, "Residential demand response for renewable energy resources in smart grid systems," *IEEE Trans. Ind. Inform.*, vol. 13, no. 6, pp. 3165–3173, Dec. 2017.
- [26] H. M. Hussain, A. Ahmad, A. Narayanan, P. H. Nardelli, and Y. Yang, "Packetized energy management controller for residential consumers," in *Proc. IEEE PES Innov. Smart Grid Technol. Eur.*, 2021, pp. 1–6.
- [27] T. Molla, B. Khan, B. Moges, H. H. Alhelou, R. Zamani, and P. Siano, "Integrated optimization of smart home appliances with cost-effective energy management system," *CSEE J. Power Energy Syst.*, vol. 5, no. 2, pp. 249–258, 2019.
- [28] P. P. Biswas, P. Suganthan, and G. A. Amaratunga, "Optimal power flow solutions incorporating stochastic wind and solar power," *Energy Convers. Manage.*, vol. 148, pp. 1194–1207, 2017.
- [29] A. Ahmad and J. Y. Khan, "Real-time load scheduling, energy storage control and comfort management for grid-connected solar integrated smart buildings," *Appl. Energy*, vol. 259, 2020, Art. no. 114208.
- [30] C. M. Colson, M. H. Nehrir, R. K. Sharma, and B. Asghari, "Improving sustainability of hybrid energy systems Part I: Incorporating battery round-trip efficiency and operational cost factors," *IEEE Trans. Sustain. Energy*, vol. 5, no. 1, pp. 37–45, Jan. 2014.
- [31] Z. Ma, S. Zou, and X. Liu, "A distributed charging coordination for large-scale plug-in electric vehicles considering battery degradation cost," *IEEE Trans. Control Syst. Technol.*, vol. 23, no. 5, pp. 2044–2052, Sep. 2015.
- [32] P. Huang, Y. Sun, M. Lovati, and X. Zhang, "Solar-photovoltaic-power-sharing-based design optimization of distributed energy storage systems for performance improvements," *Energy*, vol. 222, 2021, Art. no. 119931.
- [33] A. Cosic, M. Stadler, M. Mansoor, and M. Zellinger, "Mixed-integer linear programming based optimization strategies for renewable energy communities," *Energy*, vol. 237, 2021, Art. no. 121559.
- [34] Y. Del Valle, G. K. Venayagamoorthy, S. Mohagheghi, J.-C. Hernandez, and R. G. Harley, "Particle swarm optimization: Basic concepts, variants and applications in power systems," *IEEE Trans. Evol. Comput.*, vol. 12, no. 2, pp. 171–195, Apr. 2008.
- [35] X.-S. Yang, *Engineering Optimization: An Introduction With Metaheuristic Applications*. Hoboken, NJ, USA: Wiley, 2010.
- [36] M. Arafa, E. A. Sallam, and M. Fahmy, "An enhanced differential evolution optimization algorithm," in *Proc. 4th Int. Conf. Digit. Inf. Commun. Technol. Appl.*, 2014, pp. 216–225.
- [37] G.-S. Seo, J.-B. Baek, C.-W. Bak, H.-S. Bae, and B.-H. Cho, "Power consumption pattern analysis of home appliances for DC-based green smart home," in *Proc. KIPe Conf. Korean Inst. Power Electron.*, 2010, pp. 240–241.
- [38] I. Lütkebohle, "Finnish Meteorological Institute," 2021, Accessed: Oct. 19, 2021. [Online]. Available: <https://en.ilmati.eenlaitos.fi/open-data>
- [39] S. Nojavan, K. Zare, and B. Mohammadi-Ivatloo, "Optimal stochastic energy management of retailer based on selling price determination under smart grid environment in the presence of demand response program," *Appl. Energy*, vol. 187, pp. 449–464, 2017.